



# A comparison study on landslide prediction through FAHP and Dempster–Shafer methods and their evaluation by $P$ – $A$ plots

Maryam Mokhtari<sup>1</sup> · Zohre Hoseinzade<sup>2</sup> · Kourosh Shirani<sup>3</sup>

Received: 8 May 2019 / Accepted: 29 December 2019 / Published online: 29 January 2020  
© Springer-Verlag GmbH Germany, part of Springer Nature 2020

## Abstract

One of the important issues in identifying susceptible landslide locations is to select effective factors in the landslide of studied areas. The complexity of this issue is due to the fact that each of the factors is a part of the desired criteria, and the selection among them is a multi-criteria decision-making problem, requiring a structured and systematic approach. In the study area, the presence of large outcrops, as well as relatively thick soils formed on the formations, has caused a significant level of the province to potentially have the conditions for the movement of the tides. In addition, the situation is exacerbated by inappropriate use of natural resources, and construction of numerous rural and forest roads. In this paper, multi-criteria decision-making (MCDM) such as the fuzzy analytical hierarchy process (FAHP) and Dempster–Shafer (DeS) method was used to detect susceptible landslide locations, and output maps were verified applying the prediction–area ( $P$ – $A$ ) method for landslide purposes. The study has utilized  $P$ – $A$  plot to evaluate and compare the obtained results of FAHP and DeS methods. The results indicated that the normalized density value achieved from  $P$ – $A$  plots was significantly higher for the FAHP than the corresponding value for the DeS. In other words, FAHP, compared to DeS, resulted in the successful detection of landslide occurrences and more accurate classification of the study area.

**Keywords** Landslide · Dempster–Shafer · Fuzzy method · Prediction area plot

## Introduction

A landslide is defined as an event in which a mass of earth or rock slides down from a mountain due to sudden changes in natural conditions (Lee et al. 2018). Dislodging billions of tons of soil and rock annually, landslides are one of the natural hazards that rank the highest next to earthquakes and floods in terms of the damage they cause. The growth of population and the development of cities in mountainous areas make it necessary to recognize and mitigate the risks of this natural phenomenon (Youssef et al. 2016; Sun et al. 2018). A landslide results from the integrated and

rapid movement of sedimentary materials along hillsides. The speed and extent of the incident may be so high as to simultaneously affect even tens or hundreds of thousands of cubic meters of rock and soil, which often brings about disastrous consequences. This natural phenomenon, having occurred throughout geological ages and periods, accounts for a part of the deformation of the earth’s surface (Zhao et al. 2018; Firomsa and Abay 2018).

Considering the adverse effects of landslides on natural resources and rural/urban residential areas as well as the erosion of significant volumes of soil, it seems warranted to develop controlling and inhibiting methods, detect or zonate potential lands, and predict landslide occurrences to avoid or diminish the potential risks (Shirani et al. 2018). Accordingly, various methods have been developed, such as the multi-criteria decision-making (MCDM) method. In this method, rather than a single optimal evaluation criterion, several criteria are used.

An MCDM version is the fuzzy method, in which Buckley (1985) used fuzzy numbers to express a decision-maker’s evaluation of various criteria for each decision. Chang (1996) used triangular fuzzy numbers to introduce a new

✉ Kourosh Shirani  
k.shirani@areeo.ac.ir

<sup>1</sup> Department of Civil Engineering, Faculty of Engineering, Yazd University, Yazd, Iran

<sup>2</sup> Department of Mining Engineering, Isfahan University of Technology, Isfahan, Iran

<sup>3</sup> Soil Conservation and Watershed Management Research Department, Isfahan Agricultural and Natural Resources, Research and Education Center, AREEO, Isfahan, Iran

technique for pairwise comparisons. Triantaphyllou and Lin (1996) proposed the fuzzy multiple-decision technique based on hierarchical analysis and a model of coefficients. That technique was the closest to the ideal one. Deng (1999) introduced a simple fuzzy method to solve the problems associated with the analysis of multiple qualitative criteria. Chou and Liang (2001) presented a fuzzy multivariate decision-making model by integrating the fuzzy theory, AHP and entropy concepts to assess the performance of shipping companies. To evaluate the performance of airports, Chang et al (2003) selected the desired criteria using traditional statistical methods. They also used FAHP to determine the weight of the mentioned criteria and applied the TOPSIS technique to rank the airports based on their performance. Tang and Beynon (2005) used the FAHP method in a study to choose a race car acceptable to a car hire company. Ayas and Ozdemir (2006) presented an intelligent technique based on this method to investigate alternatives to machines. First, they used this method to weigh alternatives. Then they analyzed the head-to-head points. Another technique based on FAHP and the balanced assessment of the IT sector was introduced by Lee et al. (2008) for the Taiwanese manufacturing industry. Ertugrul and Karakasoglu (2009) used FAHP to evaluate the performance of Turkish cement companies.

Another way of multi-criteria decision-making is the Dempster–Shafer (DeS) technique introduced by Dempster (1967) and developed by Shafer (1976). The technique is associated with the Bayesian probability theory with that it transacts subjective beliefs. Therefore, DeS subsumes the Bayesian probability theory as a specific case which is not able to transact ignorance. It has extensively been applied in many different fields including artificial intelligence, expert systems, pattern recognition, information fusion, risk assessment, and multiple-attribute decision analysis (Enea and Salemi 2001; Beynon et al. 2000; Beynon 2002; Althwaynee et al. 2012; Tang 2015; Mezaal 2017; Shirani et al. 2018).

In the present research, the major geological factors that were of effect on the occurrence of landslides in the study area included large outcrops and slip-sensitive formations (e.g., Gizan schists, Shemshak formation, Khoshyyalagh formation, and Les Quaternaries) and relatively thick soils formed on those formations (Mohammady et al. 2012). Therefore, the landslide susceptibility map was evaluated based on the Fuzzy Analytic Hierarchy Process and the DeS theory. These two were chosen because they could deal with multiple decision-making problems and heterogeneous data types. FAHP was used to rate the evaluation criteria for landslide susceptibility in the fuzzy space. The DeS theory was used as it could deal with the ignored or missing information, which is very likely to occur.

The goal of the study was set to be the introduction and utilization of a  $P$ – $A$  plot to assess the FAHP and DeS methods comparatively. This could verify the prediction capability of those methods and quantify their output uncertainty. The advantage of this approach is the non-interference of expert opinions to evaluate and compare the applied methods. The outputs of the methods were, thus, objectively evaluated by means of the  $P$ – $A$  plot.

## Study area

The study area is located at a north latitude of  $36^{\circ} 50'$  and east longitude of  $54^{\circ} 25'$ . The province is bounded in the north by Turkmenistan country, in the south by Semnan province, in the east by the northern Khorasan, and in the west by the Caspian Sea and Mazandaran (Mohammady et al. 2012). Golestan province with an area of  $2043.74 \text{ Km}^2$ , occupies 1.3% of the country's total area. Its center is Gorgan city with the area of  $24.96 \text{ Km}^2$ . In terms of topography, the slope of the area is downward, and the groundwater flows from south to north. The average slope is 4%, and the two rivers flow through it (Fonooni 1989). Figures 1 and 2 depict the location of the study area in Iran and its geological map, respectively (Table 1).

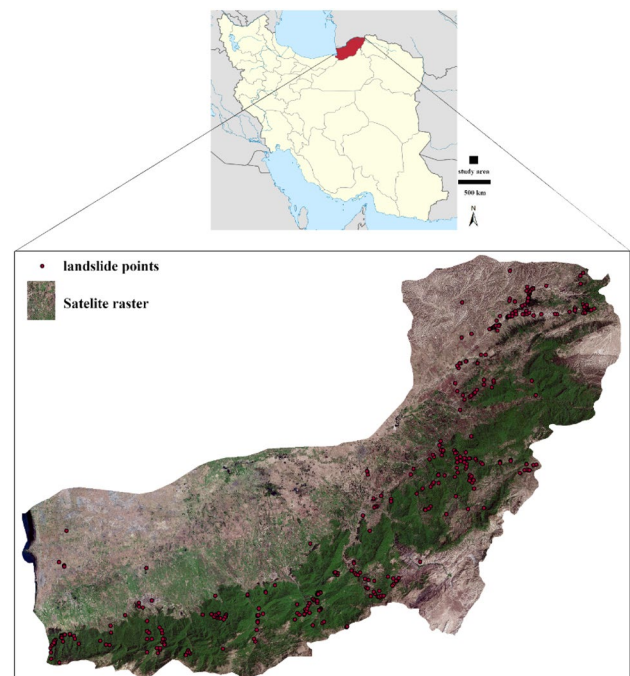


Fig. 1 Location of the study area in Iran

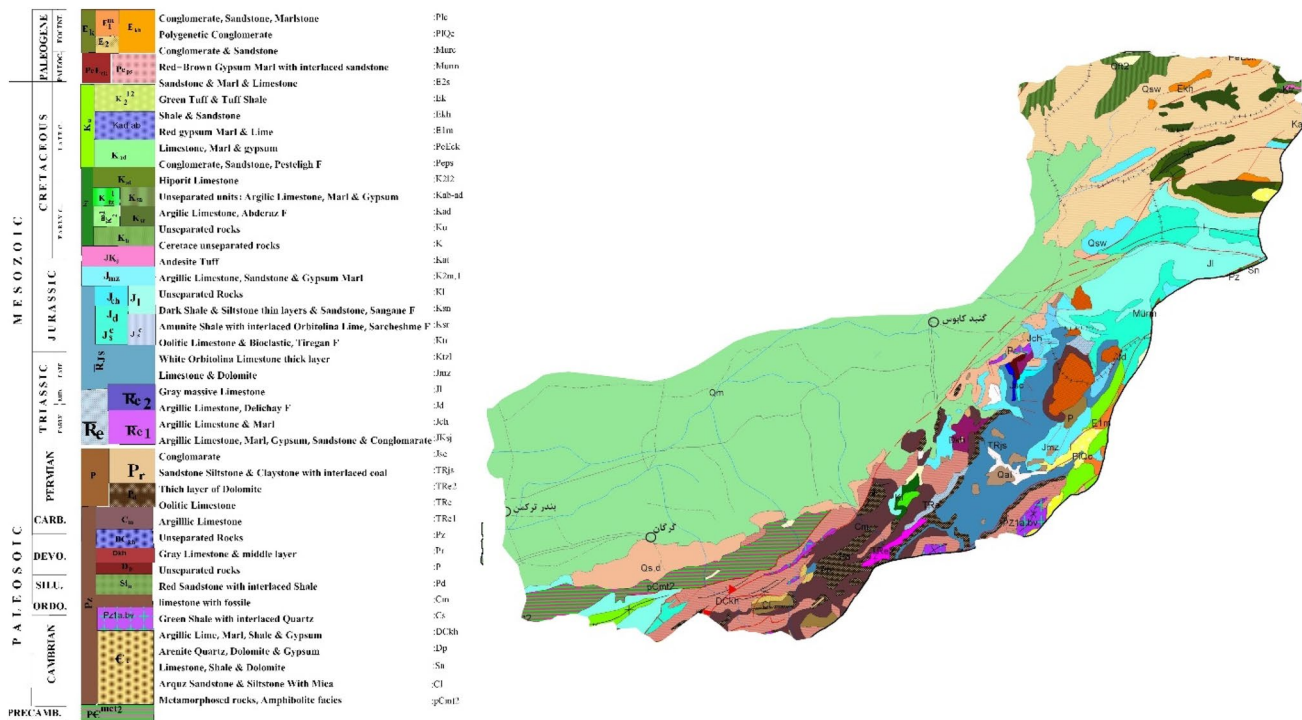


Fig. 2 Geological map of Golestan province

### Methodology

Humans have always been subjected to choosing and decision-making. Decisions include the correct expression of objectives, determination of different and possible solutions and their feasibility assessment, evaluation of the consequences and results of the implementation of each solution, and finally selection and execution. In most cases, decisions are favorable for the decision-maker when they are examined based on quantitative or qualitative multi-criteria. In multi-criteria decision-making (MCDM) approaches employed in recent decades, a multi-criteria measure is used rather than a single-criterion optimization measure (Pohekar and Ramachandran 2004).

One of the MCDM techniques is the FAHP method, which is based on the concept of the fuzzy theory. The process of fuzzy hierarchy analysis extends the AHP approach by merging it with the fuzzy set theory. In a fuzzy AHP, after creating a hierarchical structure for a problem, fuzzy relative scales are used to indicate the relative importance of the factors corresponding to the criteria. In this way, a fuzzy judgment matrix is yielded, and the final scores of the options are presented in fuzzy numbers, offering the optimal option obtained through fuzzy number ranking using certain algebraic operators (Ho et al. 2010).

Other MCDM techniques were developed based on the DeS theory. This theory, a development of the Bayesian

theory of subjective probability, is identified as the theory of belief functions. While the Bayesian theory needs probabilities for each query of interest, belief functions permit us to base degrees of belief for one query on probabilities of an associated query. These degrees of belief may or may not have the mathematical characteristics of probabilities, depending on how closely the two queries are related. The theory attracted scholars' attention in the early 1980s when the scholars were attempting to incorporate the probability theory into critic systems. Previous research has indicated that managing uncertainty intrinsically needs more structure than is available in simple rule-based systems. However, the DeS theory has remained attractive due to its relative flexibility. This theory is based on two ideas: (1) obtaining degrees of belief for one query from subjective probabilities of an associated query, and (2) the Dempster's rule for merging such degrees of belief when they are based on independent pieces of evidence (Dempster 1967; Shafer 1976; Tang, 2015).

As indicated in the flowchart (Fig. 3), the research consists of five stages as follows:

- (1) Collecting the data on eight features including Aster DEM, roads, faults, stream networks, Corine land cover, geological maps, precipitation and temperature.

**Table 1** Types of geological formation in the study area

Class	Age–era	Description
II	Paleozoic	Dark grey to black fossiliferous limestone with subordinate black shale (MOBARAK FM)
III	Paleozoic	light red to white, thick-bedded quartz arenite with dolomite intercalations and gypsum (PADEHA FM)
	Mesozoic	Grey thick-bedded limestone and dolomite (MOZDURAN FM)
	Paleozoic	Andesitic basaltic volcanic
	Mesozoic	Thick-bedded dolomite
IV	Paleozoic	Dark red medium-grained arkosic to subarkosic sandstone and micaceous siltstone ( LALUN FM)
	Mesozoic	Light grey, thin-bedded to massive limestone (LAR FM) Conglomerate Cretaceous rocks in general Lower Cretaceous, undifferentiated rocks Upper Cretaceous, undifferentiated rocks
	Paleozoic	Dark grey medium-bedded to massive limestone (RUTEH LIMESTONE) Undifferentiated lower Paleozoic rocks
	Cenozoic	Stream channel, braided channel and flood plain deposits Swamp
V	Paleozoic	Yellowish, thin- to thick-bedded, fossiliferous argillaceous limestone, dark grey limestone, greenish marl and shale, locally including gypsum
	Proterozoic	Late Proterozoic–early Cambrian undifferentiated rocks
	Cenozoic	Olive green shale and sandstone (KHANGIRAN FM)
	Proterozoic	Low-grade, regional metamorphic rocks (Green Schist Facies)
	Paleozoic	Red sandstone and shale with subordinate sandy limestone (DORUD FM) Greenish grey shale, sandstone, sandy lime, coral limestone and dolomite (NIUR FOR)
	Mesozoic	Thick-bedded grey oolitic limestone; thin, platy, yellow to pinkish shale limestone with worm tracks and well- to thick-bedded dolomite and dolomitic limestone (ELIKAH FM)
VI	Cenozoic	Marl, gypsiferous marl and limestone
	Mesozoic	Well- to thin-bedded, greenish-grey argillaceous limestone with intercalations of calcareous shale (DALICHAH FM) Dark grey shale and sandstone (SHEMESHAK FM) Undifferentiated units including argillaceous limestone, marl and shale Olive green glauconitic sandstone and shale (AITAMIR FM) Grey to black shale and thin layers of siltstone and sandstone (SANGANEH FM) Ammonite-bearing shale interacting with orbit Olin limestone (SARCHESHMEH FM)
	Cenozoic	Polymathic conglomerate and sandstone Fluvial conglomerate, piedmont conglomerate and sandstone High-level piedmont fan and valley terrace deposits
	Mesozoic	Dark grey argillaceous limestone and marl (CHAMAN BID FM)
VII	Cenozoic	Low-level piedmont fan and valley terrace deposits Light-red to brown marl and gypsiferous marl with sandstone intercalations Gypsiferous marl
	Cenozoic	Swamp and marsh
VIII	Cenozoic	Swamp and marsh
X		Unconsolidated wind-blown sand deposit including sand dunes

- (2) Testing the conditional independence of the landslide conditioning factors by overlaying every factor map on the landslide inventory map.
- (3) Testing the multi-collinearity among the data.
- (4) Providing weighted maps by means of the DeS and FAHP models.
- (5) Applying  $P$ – $A$  plots to validate and assess the two models comparatively.

Mass function is defined by the DeS theory as the relationship between input conditioning factors and the known landslides. In this study, susceptible and non-susceptible regions are distinguished by the mass function which is calculated by applying susceptibility analysis and likelihood ratio functions. The ratio of susceptible and non-susceptible regions can focus on their contrast. Layers are elected such as evidence  $E_i$  ( $i = 1, 2, \dots, l$ ) for proposed target  $T_p$  that

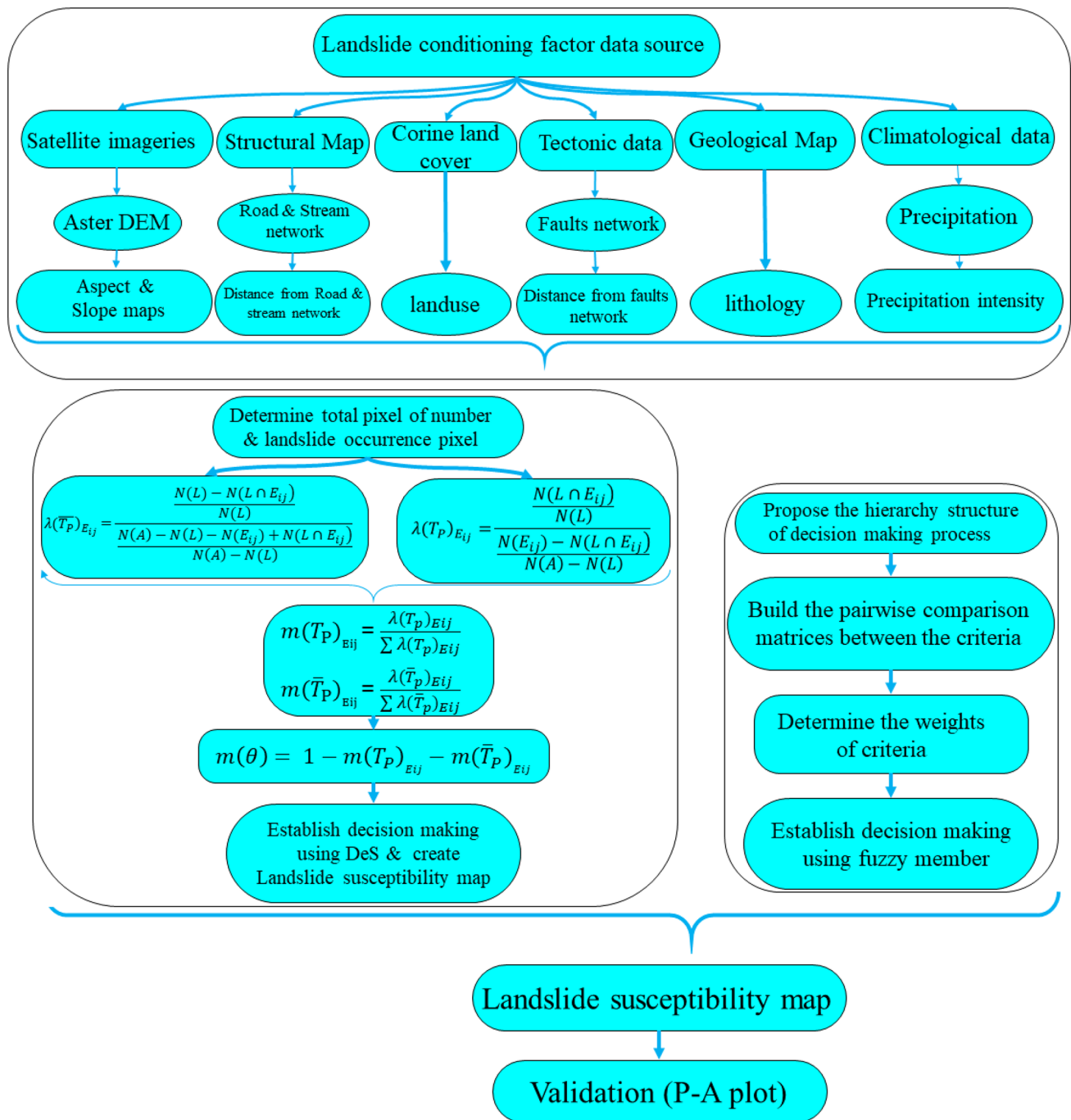


**Fig. 3** Flowchart explaining landslide susceptibility maps using MCDM methods

existed in the region. The likelihood ratio  $\lambda(T_p)E_{ij}$  for the validation of the proposed positive target has been mentioned in the flowchart. Then the ratio of non-susceptible and susceptible regions for the attribute  $E_{ij}$  is shown as the numerator and denominator. All likelihood ratio values of class attributes of the evidence  $E_i$  divide the likelihood ratios to meet the standardization condition, and to consider

relative importance within the class attribute (Shirani et al. 2018):

Mass function defines the belief function  $(m(T_p)E_{ij})$  for supporting the positive target preposition as seen in the flowchart. In addition, the belief and plausibility functions based on the likelihood ratio functions are defined using the constraints related to the occurrence of a landslide. The DeS theory is a combination of belief, disbelief, uncertainty, and

plausibility functions; therefore, it is the basis of evidence function estimation. Belief and plausibility are upper and lower boundaries of probability and the difference between belief and plausibility is defined as uncertainty function. The lack of correctness belief based on existing evidence is disbelief function. When landslides have not happened in the attribute  $E_{ij}$ , belief does not exist in the proposed target. Anyhow there is uncertainty in the landslide studies and this does not mean disbelief in its complement. Therefore,  $(m(T)E_{ij})$  and consequently  $m(\theta)E_{ij}$  are set to 0 and 1, respectively. Landslide occurrences are depending on the second complementary constraint. For example, in flat areas, it cannot apply the first constraint. Therefore, no belief exists and landslide occurrence does not happen. Although based on the first constraint the disbelief and uncertainty are set to 0 and 1, the disbelief should be set to 1 based on the second constraint. Eventually, belief and disbelief functions and uncertainty are considered, respectively, 0, 0 and 1 in this situation (Park 2011; Shirani et al. 2018) (Table 2).

Generally speaking, FAHP is performed in four steps including (1) propose the hierarchy structure of the decision-making process, (2) build the pairwise comparison matrices for the criteria, (3) determine the weights of the criteria, and (4) do the decision-making task using fuzzy members.

## Results

### Fuzzy analytical hierarchy process

This research was conducted through library and field study methods to analyze landslide zonation. Based on field

observations and expert opinion, the effective factors in the occurrence of this phenomenon were determined, and the database was prepared from the existing layers. FAHP and DeS were used to examine the factors affecting an earthquake. DeS was used because it could deal with ignorance and missing information, which is very likely in reality. FAHP is based on analyzing complex problems with hierarchical ranking, which lead to the ultimate goal. In this method, the elements of different levels are compared pairwise. Ultimately, each of the elements is valued based on their preference. Given that the number of the selected information layers in this case was 6, the ranking matrix was 7\*7 (see Tables 3, 4).

### Effective factors

#### Slope

Slope is considered one of the important and effective factors in the rupture of hillsides. Increase in a slope disturbs the equilibrium of the hillside-forming materials and increases shear stresses in hillside materials. Other factors remaining constant, the probability of sliding has a direct relation with the slope, and sliding does not occur on slopes less than 5° (Varnes 1958, 1978). In this step, the slope map was produced using a digital elevation model (DEM), and the slope of the area was clustered into five classes based on the importance of the slope in urban activities (Fig. 4a).

**Table 2** The summary of symbols used in the present study

$E_{ij}$	The $j$ th attribute class of the evidence $E_i$	$N(L \cap E_{ij})$	The number of landslide pixels occurred in $E_{ij}$
$N(E_{ij})$	The density of pixels in $E_{ij}$	$N(L)$	Total number of landslides happened in the study area
$N(A)$	The number of pixels in the whole study area $A$	$m(T_p)E_{ij}$	Belief function
$\lambda(T_p)E_{ij}$	The likelihood ratio for positive target	$\lambda(\overline{T_p})E_{ij}$	The likelihood ratio to support proposition of the opposite target
$m(\theta)E_{ij}$	Uncertainty function	$m(\overline{T_p})E_{ij}$	Disbelief function

**Table 3** Comparison of factors affecting landslide

	Land use	Slope	Distance to fault	Distance to stream	Distance to road	Precipitation	Geology
Land use	1						
Slope	5	1					
Distance to fault	5	0.5	1				
Distance to stream	7	0.33	0.5	1			
Distance to road	3	0.33	0.33	0.5	1		
Precipitation	3	0.33	0.1	0.2	0.2	1	
Geology	2	0.5	1	2	3	2	1

**Fig. 4** Characteristic factors: **a** slope map, **b** rainfall raster, **c** aspect map, **d** temperature map, **e, h** fault map, **f** drainage map, **g** road map, **i** geology map, and **j** land use map

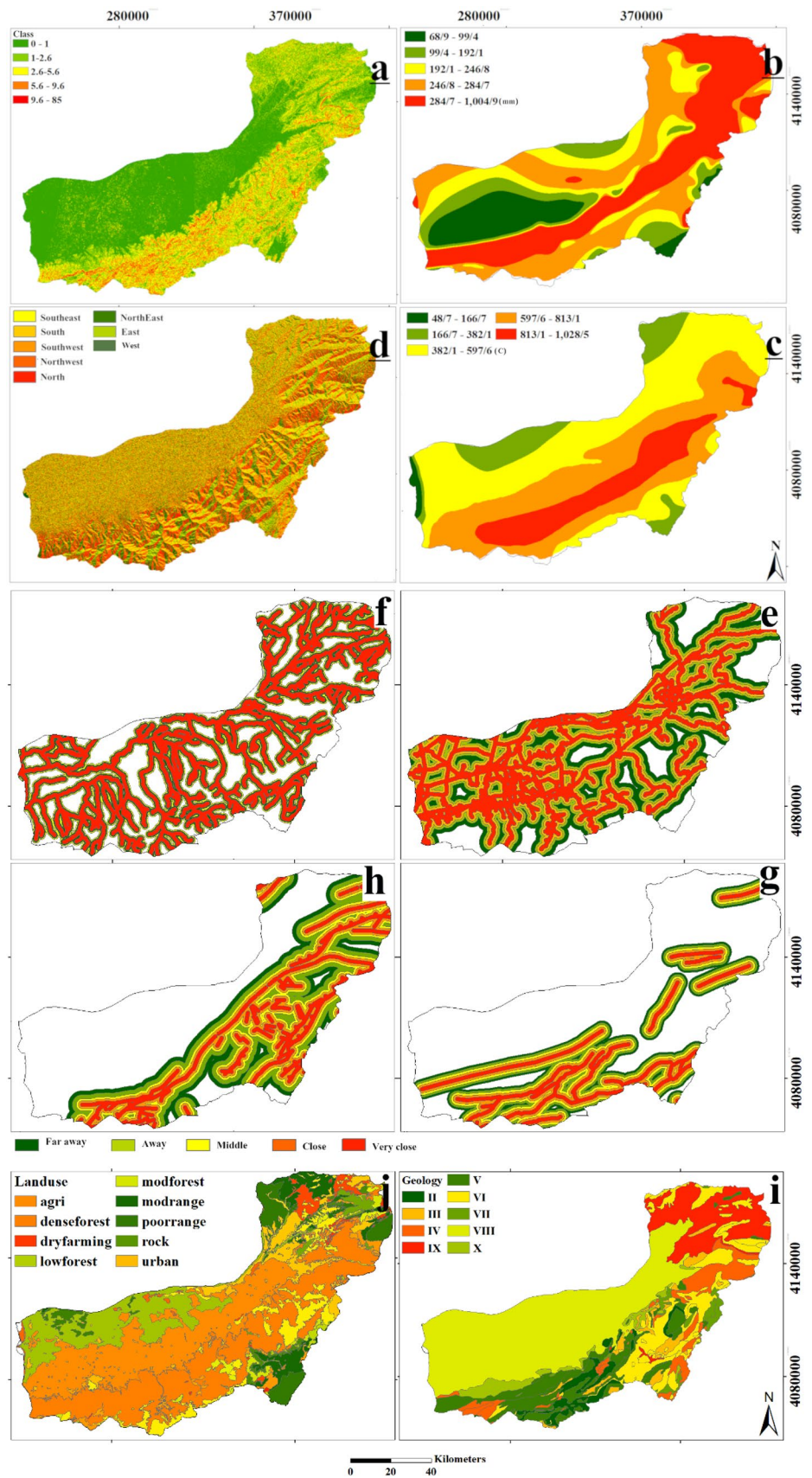


**Table 4** Weights of layers of the study area

Layers	Land use	Slope	Distance to fault	Distance to stream	Distance to road	Geology	Precipitation
Weight	0.7	0.8	0.7	0.6	0.5	0.8	0.4

### Slope aspect

This map was produced by (DEM) and mapped into eight directions including north, south, east, west, northwest, northeast, southwest and south east (Fig. 4d). Accordingly, most of the dispersion of landslides in the area had been located in the northwest and the least in the north.

### Distance to fault

The distance from the fault and the possible effect of earthquakes on landslides are very prominent factors. In general, a significant percentage of landslides in the study area have been observed near faults. The effect of faults on hillside movements is evident in different forms:

1. Earthquakes near the faults have high intensity and acceleration.
2. The impact of faults on the crushing of surrounding rocks
3. More water penetration into crushed masses, increasing the level of groundwater and pore water pressure (Varnes 1958, 1978). As the distance from major faults increases, the impact of earthquakes and the probability of occurrence of hillside instabilities decrease. Therefore, the probability of occurrence or non-occurrence of sliding instabilities can be represented in terms of the distance from faults (Fig. 4e, h).

### Distance to road

Construction of a road with numerous trenches increases shear stress and causes instability and slope sliding. Change in the geometry of the slope, which can cause instability, is one of the first measures in this operation. Many roads have been established on the hillsides of the area, which can be a factor in increasing tension in the region (Fig. 4g).

The layer of distance from the road was prepared using the topographic map of the study area, and then entered into the geographical information system and digitized. The buffer of this information layer was prepared at intervals of 1000, 2000, 3000, and 4000 for further analysis. According to the information obtained from this layer, it is clear that the highest frequency of occurrence of landslides is associated with nearby faults, and the lowest with far distant

ones. Therefore, it can be concluded that the road plays a significant role in these mass movements in that the density of mass movements in the region decreases as the distance from the road increases. This factor has somewhat increased instability due to roughness of hillsides and their slope variations.

### Distance to a stream

Generally, the occurrence of a landslide has a reverse relation with distance from a stream. Streams in the study area play a significant role in increasing the susceptibility of adjacent hillsides to instability. This layer was prepared using the topographic map of the region. The desired layer was mapped in five floors (Fig. 4f).

### Precipitation

The effect of precipitation on the instability of hillsides depends on the climatic conditions and topography of the area. Annual precipitation shows variance across different regions (Varnes 1958, 1978). The effect of precipitation is observed as a set of external dynamic functions and mechanical activities such as saturation of materials, increase in mass volume and groundwater level, and static and dynamic loads. Thus, rain stimulates a set of agents, making hillsides susceptible to sliding. Considering the shape of the iso-precipitation map in Fig. 4b, it is evident that hillside motions somewhat increase by an increase in rainfall, but from that range (284–1004 mm), the motions abruptly decrease. This could be due to the direct impact of heights on sliding movements.

### Land use

One of the factors which affect the slope instability is land use change. This factor will increase shear stress and imbalance in a short time. The conversion of forest to residential land is one of the most obvious changes in land use. Airborne photos and satellite data clarification along with field observations were applied to allocate the land cover types in the area. Nine categories of it were recognized including low forest, mod forest, dense forest, irrigated farming, dry farming, urban, poor range, midrange and rock.



**Table 5** Classified geology types

Class	Geology type	Class	Geology type
Ll	Limestone with subordinate black shale	IV	Grained arkosic to subarkosic sandstone and micaceous siltstone and massive limestone and Conglomerate
Lll	Andesitic basaltic volcanic and thick-bedded dolomite	IX	Stream channel, braided channel and flood plain deposits and swamp
V	Limestone, red sandstone, shale with subordinate sandy limestone, undifferentiated Permian rocks, limestone greenish marl, shale, locally including gypsum	Qs	Unconsolidated wind-blown sand deposit including sand dunes
Qm	Swamp and marsh	VII	Dark grey argillaceous limestone, marl, Low level piedmont fan, valley terrace deposits, gypsiferous marl with sandstone intercalations and Gypsiferous marl
VI	High-level piedmont fan and valley terrace deposits, fluvial conglomerate, ammonite-bearing shale with interaction of orbitolin limestone, grey to black shale, thin layers of siltstone and sandstone, olive green glauconitic sandstone, shale, dark grey shale, sandstone, argillaceous limestone with intercalations of calcareous shale, marl, gypsiferous marl and limestone		

## Geology

The lithology map is classified according to the rock types (Fig. 4j) (Table 5).

## Dempster–Shafer

Mass functions including belief, disbelief, and ignorance were estimated via DeS technique as shown in Table 6. The maximum values of belief function in that category related to minimum values of the disbelief and ignorance function.

## Verification of susceptibility maps

Using data from the Environmental and Natural Resources Organization and interpreting the information layers of the study area, areas susceptible to landslides were identified, and areas whose morphologies indicated landslides were marked to be reviewed. Finally, after regional and field observations, the characteristics of each landslide were recorded using GPS and planned on the map of the region.

Comparison of FAHP and DeS established that FAHP clearly identified most landslide events. The method identified as the  $P$ – $A$  diagram was utilized for quantitative assessment of outputs (Yousefi and Carranza 2015; Yousefi and Nykänen 2015). In this method, first, the accumulative percentage of the known event located in each category is calculated via a raster output classified based on predefined threshold values. At the second stage, the sector of the involved area size for each category is characterized cumulatively. Subsequently, these are depicted on the diagram in which  $X$ - and  $Y$ -axes, respectively, include threshold values and cumulative involved area sizes. By way of the sum of the prediction rate and the involved area for this point which is identical to 100, the method that delivers the landslide potential map which is most likely to detect known landslide susceptibility points is the most efficient one (Yousefi and Carranza 2015; Yousefi and Nykänen 2015). In this paper, obtained results of DeS and FAHP techniques were verified via this method. Figure 5 shows the  $P$ – $A$  plots of the present study. As it is evident in these plots, the values obtained by FAHP are significantly higher than those obtained by the DeS. FAHP resulted in a more effective classification of the study area than did DeS. In addition, FAHP successfully detected landslide occurrences (see Fig. 6).

## Discussion

Next to earthquakes and floods, landslides are known as the most hazardous natural phenomenon that causes massive damages through the displacement of billions of tons of soil and rock annually. Rapid population growth and the

**Table 6** The values obtained from the relationship between effective factors using DeS

Predisposing factor	Class	Total number of pixels	$N(L \cap E_{ij})$	$M(T_p)E_{ij}$	$M(T_p^-)E_{ij}$	$M(\theta)$
Land use	Low forest	1.78913E+11	0	0.000	0.103	0.897
	Mod forest	5.61846E+11	22	0.001	0.102	0.897
	Dense forest	2.75769E+11	252	0.021	0.051	0.928
	Irr-farming	3.24686E+09	140	0.973	0.073	-0.046
	Dry farming	3.26133E+11	70	0.005	0.090	0.905
	Urban	1.24844E+12	2	0.000036	0.113	0.887
	Poor range	6.95102E+12	0	0.000	0.242	0.758
	Midrange	2.37272E+12	8	0.000076	0.125	0.875
Geology	Rock	6.09683E+10	2	0.001	0.102	0.898
	II	5.47083E+08	45	0.253	0.063	0.683
	III	4.19161E+08	12	0.088	0.069	0.843
	IV	1.23771E+09	21	0.052	0.068	0.880
	IX	1.47186E+11	63	0.001	0.487	0.511
	V	2.00652E+09	155	0.238	0.045	0.717
	VI	2.62711E+09	57	0.067	0.062	0.871
	VII	8.35171E+08	20	0.074	0.068	0.859
	VIII	1.25322E+10	17	0.004	0.073	0.923
	X	4.70986E+08	34	0.222	0.065	0.713
Distance to fault	< 1000	2.90996E+09	88	0.362	0.166	0.471
	1000–2000	2.66018E+09	46	0.161	0.210	0.629
	2000–3000	2.32574E+09	26	0.104	0.220	0.676
	3000–4000	3.01265E+09	38	0.118	0.224	0.658
	> 4000	4.54455E+09	91	0.187	0.207	0.606
Distance to stream	< 1000	5.09299E+09	88	0.176	0.208	0.615
	1000–2000	2.03868E+09	52	0.227	0.191	0.581
	2000–3000	1.63914E+09	50	0.272	0.186	0.542
	3000–4000	2.54455E+09	24	0.084	0.223	0.693
	> 4000	3.54455E+09	75	0.189	0.198	0.614
Distance to road	< 1000	9.23520E+06	91	0.995	0.134	-0.129
	1000–2000	4.18287E+09	57	0.001	0.226	0.773
	2000–3000	2.59610E+09	32	0.001	0.214	0.784
	3000–4000	1.90488E+09	21	0.001	0.211	0.788
	> 4000	5.05890E+09	88	0.002	0.215	0.783
Precipitation	48–264	3.85591E+06	0	0.000	0.196	0.804
	264–361	3.90901E+09	0	0.000	0.301	0.699
	361–497	3.39854E+09	144	0.236	0.174	0.590
	497–674	2.29822E+09	55	0.133	0.210	0.657
	674–1029	1.57130E+09	178	0.631	0.120	0.249
Slope	0–15	3.12419E+07	2	0.035	0.209	0.756
	15–30	1.13109E+08	15	0.073	0.230	0.697
	30–45	1.26805E+08	82	0.354	0.178	0.468
	45–60	1.74151E+08	89	0.280	0.189	0.531
	> 60	2.13784E+08	101	0.259	0.193	0.548

**Table 6** (continued)

Predisposing factor	Class	Total number of pixels	$N(L \cap E_{ij})$	$M(T_p)E_{ij}$	$M(T_p^-)E_{ij}$	$M(\theta)$
Slope aspect	Flat	1.12183E+07	0	0.000	0.113	0.887
	North	1.15357E+08	16	0.035	0.125	0.840
	Northeast	8.13175E+07	75	0.232	0.093	0.675
	Northwest	1.12004E+08	91	0.205	0.090	0.705
	South	8.13766E+07	15	0.046	0.119	0.835
	Southeast	2.31886E+07	19	0.206	0.107	0.687
	Southwest	3.12731E+07	21	0.169	0.108	0.723
	West	1.13015E+08	23	0.051	0.122	0.827
	East	1.31941E+08	29	0.055	0.123	0.822

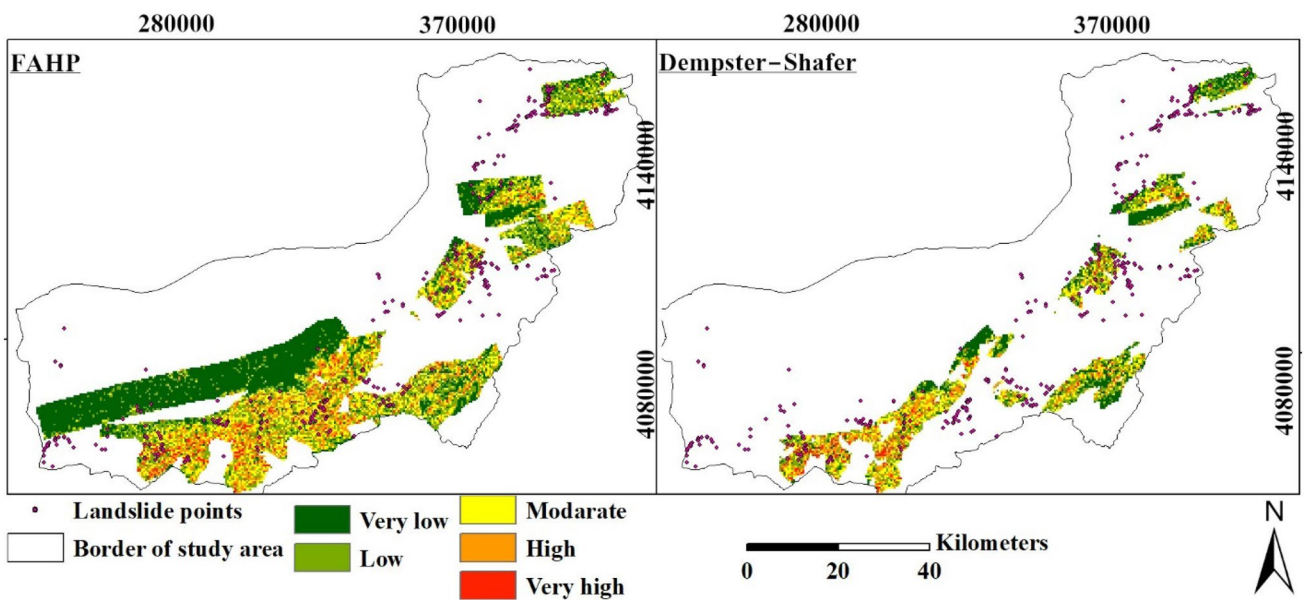


**Fig. 5** Landslide susceptibility zonation maps obtained using MCDM methods

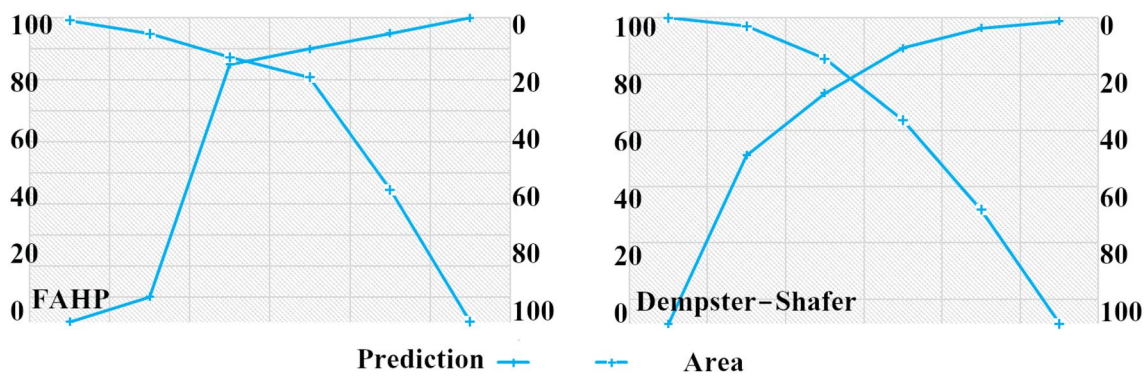


**Fig. 6** Prediction–area plots of maps obtained by MCDM methods

development of cities in mountainous areas make it necessary to identify and mitigate the risks of this natural phenomenon. Landslides result from the integrated and rapid movement of sedimentary materials along hillsides. The damage they make depends on their speed and extent. They may be so large as to simultaneously move hundreds of thousands of cubic meters of rock and soil. This phenomenon has, thus, deformed the surface of the earth throughout geological periods. Nowadays, experts take landslide events into careful consideration, and producing exact maps of landslide occurrence has become a current concern in geology (Chen et al. 2016; Lee et al. 2018).

In this research, the potential of the DeS and FAHP methods was assessed in the study area in Golestan Province, Iran. As the first step, extensive landslide inventory mapping was done on the account that a reliable landslide inventory map is generally necessary for indirect landslide susceptibility evaluations. In the second stage, the landslide conditioning factors were determined for the evaluation of the area susceptibility through DeS and FAHP models. Finally, a *P–A* plot was produced based on a set of data randomly collected from landslide spots and safe zones. The experimental results of this case study illustrated that the proposed scheme based on DeS and FAHP models can adequately account for the quantitative relationship between landslide occurrence and multiple spatial data layers. The validation results also showed that the occurrences in the area under the curve in DeS and FAHP models could be predicted with the accuracy of 0.79 (79%) and 0.85 (85%), respectively. In other words, the predictability of landslides by FAHP mapping was slightly higher than that by the DeS model.

## Conclusion

Valuation of landslide susceptibility is highly important for handling potentially susceptible areas. Scholars attempt to improve and use easy, user-friendly and understandable models capable of making results more compatible with landslide events. These models should create near realistic predictions for landslide-susceptible zones. In this paper, we presented an integrated decision-making approach based on the fuzzy analytical hierarchy process and the Dempster–Shafer theory for evaluating landslide susceptibility in Gorgan province, and the outputs were compared using the *P–A* plot. The FAHP approach provides a pliable technique that includes a connoisseur’s viewpoint on creation of an inference system though the DeS belief model applies mixture laws, where a connoisseur only can allocate belief functions to each factor map category. Typically, fuzzy systems can be applied in different ways to model two main types of uncertainty: (1) uncertainty from the lack of knowledge and human tools for understanding the complexities of a

phenomenon, and (2) uncertainty associated with inaccuracy and the lack of transparency related to a particular phenomenon or its specific features. Fuzzy logic with extreme flexibility in analyzing natural language meanings is able to model and analyze ambiguities pertaining to the human mind and the environment, and the uncertainty that always exists in human judgment. Thus, the results of the present study have practical implications for managers’ policy-making, planning, and decision-making. Overlaying sliding locations on each of the first seven layers indicated that most landslides occur on 12–30% slopes and in the south direction due to its weaker vegetation.

Investigating the effective factors on landslides indicated that the central part of the study area is most sensitive to slides. Considering the man-made fractures and the resulting environmental disruptions, road intersections are susceptible areas for slides. The presence of streams causes pipping and increases the possibility of slide occurrence. In addition, most slides occur in areas with 500–700 mm precipitation. Lithological and soil studies have indicated that most slides occur in silt–clay–loam soils. This can be due to higher water absorption and lower hydraulic penetration of soils with medium and fine textures as a result of easier saturation. Generally, the obtained maps can be used to identify high-risk areas and develop ways to prevent this natural destructive phenomenon.

## References

- Althuwaynee OF, Pradhan B, Lee S (2012) Application of an evidential belief function model in landslide susceptibility mapping. *Comput Geosci* 44:120–135
- Ayas Z, Ozdemir RG (2006) A fuzzy AHP approach to evaluating matching tool alternatives. *J Intell Manuf* 17:179–190
- Beynon MJ (2002) An investigation of the role of scale values in the DS/AHP method of multi-criteria decision making. *J Multi Criteria Decis Anal* 11(6):327–343
- Beynon M, Curry B, Morgan P (2000) The Dempster–Shafer theory of evidence: an alternative approach to multi criteria decision modelling. *Omega* 28(1):37–50
- Buckley JJ (1985) Fuzzy hierarchical analysis. *Fuzzy Sets Syst* 17:233–247
- Chang DY (1996) Applications of the extent analysis method on fuzzy AHP. *Eur J Oper Res* 95:649–655
- Chang YH, Cheng CH, Wang TC (2003) Performance evaluation of international airports in the region of east Asia. *Proc East Asia Soci Transp Stud* 4:213–230
- Chen W, Wang J, Xie X, Hong H, Van Trung N, Bui DT, Li X (2016) Spatial prediction of landslide susceptibility using integrated frequency ratio with entropy and support vector machines by different kernel functions. *Environ Earth Sci* 75(20):1344
- Chou TY, Liang GS (2001) Application of a fuzzy multi-criteria decision making model for shipping company performance evaluation. *Marit Policy Manag* 28(4):375–392
- Dempster AP (1967) Upper and lower probabilities induced by a multi valued mapping. *Ann Math Stat* 28:325–339

- Deng H (1999) Multi criteria analysis with fuzzy pair-wise comparison. *Int J Approx Reason* 21:215–231
- Enea M, Salemi G (2001) Fuzzy approach to the environmental impact evaluation. *Ecol Model* 135:131–147
- Ertugrul I, Karakasoglu N (2009) Performance evaluation of Turkish cement firms with fuzzy analytic hierarchy process and TOPSIS methods. *Expert Syst Appl* 36:702–715
- Firomsa M, Abay A (2018) Landslide assessment and susceptibility zonation in Ebantu district of Oromia region, western Ethiopia. *Bull Eng Geol Environ* 78:1–11
- Fonooni B (1989) Investigating the causes of water level decline in the city of Gorgan. Irrigation Department, Kannur
- Ho W, Xu X, Dey PK (2010) Multi-criteria decision making approaches for supplier evaluation and selection: a literature review. *Eur J Oper Res* 202(1):16–24
- Lee AH, Chen WC, Chang CJ (2008) A fuzzy AHP and BCS approach for evaluating performance of IT department in the manufacturing industry in Taiwan. *Expert Syst Appl* 34:96–107
- Lee S, Lee MJ, Lee S (2018) Spatial prediction of urban landslide susceptibility based on topographic factors using boosted trees. *Environ Earth Sci* 77(18):656
- Mezaal MR, Pradhan B, Shafri HZM, Yusoff ZM (2017) Automatic landslide detection using Dempster–Shafer theory from LiDAR-derived data and orthophotos. *Geomat Nat Hazards Risk* 8(2):1935–1954
- Mohammady M, Pourghasemi HR, Pradhan B (2012) Landslide susceptibility mapping at Golestan Province, Iran: a comparison between frequency ratio, Dempster–Shafer, and weights-of-evidence models. *J Asian Earth Sci* 61:221–236
- Park NW (2011) Application of Dempster–Shafer theory of evidence to GIS-based landslide susceptibility analysis. *Environ Earth Sci* 62(2):367–376
- Pohekar SD, Ramachandran M (2004) Application of multi-criteria decision making to sustainable energy planning—a review. *Renew Sustain Energy Rev* 8(4):365–381
- Shafer G (1976) A mathematical theory of evidence. Princeton University Press, Princeton
- Shirani K, Pasandi M, Arabameri A (2018) Landslide susceptibility assessment by Dempster–Shafer and Index of Entropy models, Sarkhoun basin Southwestern Iran. *Nat Hazards* 93(3):1379–1418
- Sun HY, Wu X, Wang DF, Liang X, Shang YQ (2018) Analysis of deformation mechanism of landslide in complex geological conditions. *Bull Eng Geol Environ* 78:1–13
- Tang H (2015) A novel fuzzy soft set approach in decision making based on grey relational analysis and Dempster–Shafer theory of evidence. *Appl Soft Comput* 31:317–325
- Tang Y, Beynon MJ (2005) Application and development of a fuzzy analytic hierarchy process within a capital Investment study. *J Econ Manag* 1(2):207–230
- Triantaphyllou E, Lin CT (1996) Development and evaluation of five fuzzy multi-attribute decision-making methods. *Int J Approx Reason* 14:281–310
- Varnes DJ (1958) Landslide types and processes. *Landslides Eng Pract* 24:20–47
- Varnes DJ (1978) Slope movement types and processes. *Spec Rep* 176:11–33
- Yousefi M, Carranza EJM (2015) Prediction-area ( $P-A$ ) plot and  $C-A$  fractal analysis to classify and evaluate evidential maps for mineral prospectivity modeling. *Comput Geosci* 79:69–81
- Yousefi M, Nykänen V (2015) Data-driven logistic-based weighting of geochemical and geological evidence layers in mineral prospectivity mapping. *J Geochem Explor* 164:94–106
- Youssef AM, Pourghasemi HR, El-Haddad BA, Dhahry BK (2016) Landslide susceptibility maps using different probabilistic and bivariate statistical models and comparison of their performance at Wadi Itwad Basin, Asir Region, Saudi Arabia. *Bull Eng Geol Environ* 75(1):63–87
- Zhao GW, Jiang YJ, Qiao JP, Yang ZJ, Ding PP (2018) Numerical and experimental study on the formation mode of a landslide dam and its influence on dam breaching. *Bull Eng Geol Environ* 78:1–15

**Publisher's Note** Springer Nature remains neutral with regard to jurisdictional claims in published maps and institutional affiliations.